Redox Biology 53 (2022) 102336

Contents lists available at ScienceDirect

Redox Biology

journal homepage: www.elsevier.com/locate/redox

BAP1 phosphorylation-mediated Sp1 stabilization plays a critical role in cathepsin K inhibition-induced C-terminal p53-dependent Bax upregulation

Seung Un Seo [a,1], Seon Min Woo [a,1], Seul Gi Lee [a], Min Yeong Kim [b], Hyun Shik Lee [c], Yung Hyun Choi [b], Sang Hyun Kim [d], Young-Chae Chang [e], Kyoung-jin Min [f], Taeg Kyu Kwon [a,g,*]

[a] Department of Immunology, School of Medicine, Keimyung University, Daegu, 42601, South Korea
[b] Department of Biochemistry, College of Korean Medicine, Dong-Eui University, Busan, 47227, South Korea
[c] School of Life Sciences, BK21 Plus KNU Creative BioResearch Group, College of Natural Sciences, Kyungpook National University, Daegu, 41566, South Korea
[d] Department of Pharmacology, School of Medicine, Kyungpook National University, Daegu, 41944, South Korea
[e] Research Institute of Biomedical Engineering and Department of Medicine, Catholic University of Daegu School of Medicine, Daegu, 42472, South Korea
[f] New Drug Development Center, Daegu-Gyeongbuk Medical Innovation Foundation (DGMIF), Daegu, 41061, South Korea
[g] Center for Forensic Pharmaceutical Science, Keimyung University, Daegu, 42601, South Korea

ARTICLE INFO

Keywords:
Odanacatib
Bax
p53
Sp1
BAP1
Mitochondrial ROS

ABSTRACT

Cathepsin K inhibitor (odanacatib; ODN) and cathepsin K knockdown (siRNA) enhance oxaliplatin-induced apoptosis through p53-dependent Bax upregulation. However, its underlying mechanisms remain unclear. In this study, we elucidated the mechanism behind enhancement of oxaliplatin-induced apoptosis by ODN. We also investigated the molecular mechanisms of ODN-induced Bax upregulation. Here, we demonstrated that ODN-induced Bax upregulation required p53, but it was independent of p53 transcriptional activity. Various mutants of the DNA-binding domain of p53 induced Bax upregulation in ODN-treated cells. p53 functional domain analysis showed that the C-terminal domain of p53 participates in the physical interaction and stabilization of Sp1, a major transcription factor of Bax. We screened a specific siRNA encoding 50 deubiquitinases and identified that BAP1 stabilizes Sp1. The knockdown or catalytic mutant form of BAP1 abolished the ODN-induced upregulation of Sp1 and Bax expression. Mechanistically, ODN induced BAP1 phosphorylation and enhanced Sp1-BAP1 interaction, resulting in Sp1 ubiquitination and degradation. Interestingly, ODN-induced BAP1 phosphorylation and DNA damage were modulated by the production of mitochondrial reactive oxygen species (ROS). Mitochondrial ROS scavengers prevented DNA damage, BAP1-mediated Sp1 stabilization, and Bax upregulation by ODN. BAP1 downregulation by siRNA inhibited apoptosis induced by the combined treatment of ODN and oxaliplatin/etoposide. Therefore, Sp1 is a crucial transcription factor for ODN-induced Bax upregulation, and Sp1 stabilization is regulated by BAP1.

1. Introduction

Cathepsin K is a papain-like cysteine protease that has high matrix-degrading activity, which supports its role in cancer invasion and progression [1–3]. It also plays a crucial role in bone resorption and has become an important target for osteoporosis treatment [4,5]. Odanacatib (ODN), a small molecule that selectively inhibits cathepsin K, has been widely investigated for osteoporosis treatment [6]. ODN exerts anti-metastatic activity by decreasing the expression of matrix metalloproteinase-9 (MMP-9) and upregulating TIMP-1 expression [7]. Cathepsin K expression and activity are associated with the mTOR signaling pathway. The pharmacologic inhibitor of mTORC1 inhibits osteoclast formation and suppresses the expression of osteoclast-specific genes, such as the gene encoding cathepsin K [8]. ODN significantly reduces mTOR phosphorylation at S2448 [9]. It also sensitizes apoptosis mediated by sublethal doses of anticancer drugs through the upregulation of USP27x-mediated Bim expression [9]. ODN and cathepsin K knockdown enhance oxaliplatin-induced apoptotic cell death through p53-dependent Bax upregulation [10]. ODN-induced p53 stabilization is attributed to casein kinase 2 (CK2)-mediated phosphorylation of OTUB1 at Ser 16 [10].

Bax is a pro-apoptotic protein that triggers the apoptotic cascade.

* Corresponding author., Keimyung University, 1095 Dalgubeoldaero, Dalseo-Gu, Daegu, 42601, South Korea.
E-mail address: kwontk@dsmc.or.kr (T.K. Kwon).
[1] These authors contributed equally to the present study.

https://doi.org/10.1016/j.redox.2022.102336
Received 14 March 2022; Received in revised form 29 April 2022; Accepted 9 May 2022
Available online 13 May 2022

The tumor suppressor protein p53 directly regulates the *Bax* promoter, which has a response element containing two consensus p53 half-sites [11,12]. Transcriptional regulation of *Bax* is modulated by several transcription factors, including p53, p73, and Sp1 [11–13]. Thornborrow et al. reported that p53 requires the cooperation of Sp1 or a Sp1-like factor to activate the transcription of *Bax* [12].

In this study, we aimed to understand how ODN enhances oxaliplatin-induced apoptosis and elucidate the molecular mechanisms of ODN-induced Bax upregulation. Our results revealed no association between Bax upregulation and p53 transcriptional activity. The C-terminal domain of p53 induced Sp1 stability through the phosphorylation of BAP1 deubiquitinase (DUB) and thus played a critical role in ODN-induced Bax upregulation.

2. Materials and methods

2.1. Cell culture and materials

All human cancer cells used in this study (Caki-1, ACHN, MDA-MB231, U251MG, and HCT116 p53 null) were obtained from the American Type Culture Collection (Manassas, VA). They were cultured in Dulbecco's modified Eagle's medium containing 10% fetal bovine serum (Welgene, Gyeongsan, Korea), 1% penicillin–streptomycin, and 100 μg/mL gentamycin (Thermo Fisher Scientific, Waltham, MA). Details of the reagents are provided in Supplementary Table 1.

2.2. Transfection

The cells were transiently transfected with siRNA or plasmids using Lipofectamine RNAiMAX (Thermo Fisher Scientific) or Lipofector p-MAX (AptaBio, Korea), respectively. Details of the siRNAs are provided in Supplementary Table 2.

2.3. Quantitative polymerase chain reaction

Total RNA was isolated using the TriZol (Life Technologies; Gaithersburg, MD, USA) and cDNA was obtained using M-MLV reverse transcriptase (Gibco-BRL; Gaithersburg, MD, USA). For qPCR, SYBR Fast qPCR Mix (Takara Bio Inc., Shiga, Japan) was used, and reactions were performed on a Thermal Cycler Dice® Real Time System III (Takara Bio Inc). We calculated the threshold cycle number (Ct) of each gene using actin as the reference gene, and we reported the delta-delta Ct values of the genes. Sequences of the primers are detailed in Supplementary Table 2.

2.4. Western blotting

For protein isolation, the cells were lysed using RIPA buffer containing a protease inhibitor [14], and the cell lysate was centrifuged at 13,000×*g* and 4 °C for 15 min. The isolated protein was separated using SDS-PAGE and transferred onto nitrocellulose membranes (GE Healthcare Life Science, Pittsburgh, PA). Protein bands were detected using an enhanced chemiluminescence kit (EMD Millipore, Darmstadt, Germany). Details of the antibodies are provided in Supplementary Table 1.

2.5. Measurement of promoter activity

The cells (Caki-1 and HCT116 p53 null) were transfected with the pGL3-Bax-luciferase plasmid using Lipofector p-MAX (AptaBio, Korea). For protein isolation, the cells were lysed using lysis buffer (25 mM Tris-phosphate, pH 7.8, 2 mM EDTA, 1% Triton X-100, and 10% glycerol) containing 1 mM PMSF, and the cell lysate was centrifuged at 13,000×*g* and 4 °C for 15 min. The lysate (30 μg) was then incubated with the luciferase substrate luciferin and measured the luciferase activity according to the manufacturer's instructions (Promega, Madison, WI, USA).

2.6. Immunoprecipitation

Immunoprecipitation was performed in accordance with a previously described method to examine protein–protein interactions [15]. Briefly, the cells were lysed in CHAPS lysis buffer and incubated with a primary antibody overnight at 4 °C. Next, the lysate was incubated with protein G agarose beads at 4 °C for 2 h. After centrifugation at 13,000×*g* for 15 min, the supernatant was removed, mixed in 2X sample buffer, and then boiled. Protein interaction was detected by western blotting.

2.7. Ubiquitination assay

Ubiquitination assay was performed using a tagged-ubiquitin plasmid pretreated with proteasome inhibitor (MG132) [16]. Briefly, the cells were harvested, washed with phosphate-buffered saline (PBS) containing 10 mM N-ethylmaleimide (NEM; EMD Millipore, Darmstadt, Germany), resuspended in 90 μL PBS/NEM containing 1% SDS, and boiled at 95 °C for 10 min. The lysate was added to the lysis buffer containing 1 mM PMSF and 5 mM NEM, resuspended using l mL syringe three to four times, and centrifuged at 13,000×*g* and 4 °C for 10 min. The obtained supernatant was incubated with the primary antibody of the target protein overnight, then incubated with protein G agarose beads at 4 °C for 2 h. After centrifugation, the supernatant was removed, washed twice with lysis buffer containing 1 mM PMSF and 5 mM NEM, mixed in 2X sample buffer, and then boiled for 10 min. Ubiquitinated Sp1 was detected using HRP-conjugated anti-Ub.

2.8. Immunofluorescence staining

Cells were fixed by 4% paraformaldehyde at 4 °C for 25 min, and permeabilized by 0.1% Triton X-100 for 2 min. After blocking with 0.1% BSA in PBS for 1 h, cells were stained with corresponding primary antibodies at 4 °C for overnight. After removing the unattached antibodies, and incubated with secondary antibodies [Alexa Fluor (AF) 488 or 555] at the room temperature for 60 min. And then cells were mounted with ProLong™ Gold Antifade Mountant with DAPI (Thermo Fisher Scientific). Fluorescence was captured by fluorescence microscope (Carl Zeiss, Oberkochen, Germany). Dilutions for primary antibodies were as follows: phosphor-BAP1 (1:300) and Sp1 (1:300).

2.9. In situ proximity ligation assay (PLA)

For the in situ visualization of protein–protein interactions, we performed the Duolink PLA Fluorescence Protocol using the Duolink® In Situ Red Starter Kit Mouse/Rabbit (Sigma-Aldrich, St. Louis, MO, USA). Briefly, fixed cells were incubated with primary antibodies at 4 °C for overnight after blocking for 1 h at 37 °C. Following washing, cells were incubated with PLA probe for 1 h at 37 °C, the ligase for 1 h at 37 °C, and polymerase at 37 °C for overnight. Finally, cells were washed and mounted with ProLong™ Gold Antifade Mountant with DAPI. Fluorescence images was analyzed by Confocal Laser Microscope (Carl Zeiss).

2.10. Measurement of ROS production in zebrafish larvae

From ~3 days post-fertilization (dpf), embryos (n = 25) were transferred to individual wells of a 24-well plate and maintained in embryo media containing sterile distilled water (control), 5 mM NAC or 2 μM Mito-TEMPO for 1 h followed by the treatment with 2 μM ODN for up to 4 dpf. The generation of ROS in the zebrafish larvae was analyzed using fluorescent probe dyes, DCF-DA or MitoSOX. After 4 dpf, the larvae were transferred to 24-well plates and incubated with DCF-DA or MitoSOX dyes for 1 h in the dark at 28.5 °C, and then anaesthetized using 1-phenoxy-2-propanol (1:500 dilution, Acros Organics, Morris Plains, NJ, USA). The images of stained larvae were observed for the ROS generation under a fluorescence microscope, and the fluorescence intensity of individual larvae was quantified ImageJ software.

2.11. Comet assay

The extent of DNA damage was analyzed using a comet assay as described [17]. In brief, the collected cells were washed with PBS, suspended in low melting agarose (LMA) at 37 °C and then spread on microscope slides, which were precoated with normal melting agarose. After the agarose are solidified, the slides were covered with LMA and then submerged in lysis solution at 4 °C for 1 h, incubated in a gel electrophoresis device for 30 min, and electrophoresed for 20 min at 30 V and 300 m Amp. And then the slides were washed with neutralizing buffer and stained with propidium iodide (PI) (20 μg/ml). The resulting nuclear images were visualized and captured using a fluorescence microscope (Carl Zeiss, Oberkochen, Germany).

2.12. Determination of 8-hydroxy-2′-deoxyguanosine (8-OHdG) concentration

The quantity of 8-OHdG in the DNA was determined using an 8-OHdG-ELISA kit according to the kit instructions. The cells were extracted cellular DNA using the Genomic DNA purification kit and adjusted to the final concentration at 200 μg/ml in each sample. Then, DNA was digested by DNase I and alkaline phosphatase sequentially for 1 h at 37 °C. For the determination of 8-OHdG in culture supernatants, the amount of 8-OHdG was quantified using an ELISA plate reader at 450 nm based on the manufacturer's instruction.

2.13. Flow cytometry analysis

The trypsinyzed cells were resuspended in 100 μL PBS and fixed using 200 μL of 95% ethanol at 4 °C. After 1 h, the cells were washed with PBS, resuspended in 1.12% sodium citrate buffer (pH 8.4) containing 12.5 μg of RNase, and incubated at 37 °C for 30 min. Then, 250 μL of PI (50 μg/mL) was added to the cells, and the cells were incubated at 37 °C for 30 min. The number of apoptotic cells was measured using a BD Accuri™ C6 flow cytometer (BD Biosciences, San Jose, CA).

2.14. Statistical analysis

Statistical analyses were performed using Statistical Package for Social Science (SPSS, Version 26.0; IBM SPSS, Armonk, NY, USA). All experiments were repeated at least three times. Data are presented as mean ± SD, and was analyzed using one-way ANOVA and post hoc comparisons (Student–Newman–Keuls).

3. Results

3.1. Cathepsin K inhibitor induces Bax upregulation

We previously reported that ODN induces p53-dependent Bax upregulation [10]. Interestingly, in the present study, ODN did not affect the protein and mRNA expression of p53 targets (p21, PUMA, and Noxa). However, etoposide, a DNA-damaging anticancer drug, induced the upregulation of all tested proteins (Bax, p21, PUMA, and Noxa; Fig. 1A). We focused on the functional role of p53 in ODN-induced Bax upregulation. We examined the effect of wild-type (WT) and mutant (R273H, it is located in DNA binding domain) p53 on ODN-induced Bax upregulation in p53-null HCT116 cells. ODN did not induce Bax expression in p53-null HCT116 cells. Interestingly, transfection with WT and mutant (R273H) p53 significantly increased the protein expression and promoter activity of Bax in ODN-treated cells compared to that in ODN-untreated cells (Fig. 1B). ODN also upregulated p53 and Bax expression in mutant p53 cancer cell lines [MDA-MB231 (R280K) and U251MG (R273H); Fig. 1C]. However, etoposide only increased Bax, p21, and p53 expression levels in WT p53 cancer cells (Caki-1) but not in mutant p53 cancer cells (Fig. 1D). The p53 inhibitors, Pifithrin-α and Pifithrin-μ, specifically block the transcriptional activity of the tumor suppressor p53 [18,19]. In our study, two p53 inhibitors significantly inhibited etoposide-induced Bax promoter activity relies on the p53 binding domain, but did not exhibit any such effects in ODN-mediated Bax promoter activation (Fig. 1E). To prove the irrelevant of p53 transcriptional activity in Bax expression by ODN, we mutated p53-binding site of Bax promoter. ODN increased regardless of p53 binding site mutation, but etoposide only induced an increase in promoter activity in theBax WT promoter (Fig. 1F). We analyzed transcriptionally inactive forms of various mutants of p53 (R125H, R245H, R248H, R272H, and R273H) that induces Bax upregulation in ODN-treated p53-null HCT116 cells. Conversely, etoposide only upregulated Bax expression in WT p53-transfected cells (Fig. 1G). Therefore, ODN-induced Bax upregulation was essential for p53 but was independent of the p53 transcriptional activity.

3.2. Sp1 is a key determinant of p53-mediated Bax upregulation

Genome-wide shRNA screening revealed Sp1 as a crucial determinant of p53-mediated apoptosis [20]. The human Bax promoter responds directly to Sp1 or cooperates with p53 and Sp1 [12,21]. We investigated the effects of Sp1 on ODN-induced Bax upregulation in this study. ODN markedly induced Sp1 expression in a time-dependent manner (Fig. 2A). The pharmacologic inhibition (mithramycin A) and siRNA-mediated knockdown of Sp1 markedly inhibited ODN-induced p53 and Bax expression in WT p53 Caki-1 and ACHN cells (Fig. 2B and C). Furthermore, transfection with the WT and mutant p53 (R273H) induced the upregulation of Bax and Sp1 in ODN-treated p53-null HCT116 cells. However, etoposide did not induce the upregulation of Sp1, Bax, and p53 in mutant p53 (R273H)-transfected cells (Fig. 2D). Therefore, Sp1 upregulation contributed to WT p53-and mutant p53-mediated Bax upregulation in ODN-treated cells.

3.3. C-terminal domain of p53 exerts ODN-induced upregulation of Bax and Sp1

Considering that the transfection of DNA-binding mutant (R273H) p53 upregulated Sp1 expression, we speculated that p53 regulates Sp1 stability. To elucidate the underlying mechanism of p53 in modulating Sp1 stability, we analyzed the role of the functional domain of p53 in Sp1 regulation. We generated three p53 deletion constructs, namely, DNA-binding core domain (CD, residues 93–292), N-terminal domain (residues 1–292), and C-terminal domain (residues 293–393; Fig. 3A). Transfection with the WT and C-terminal domain of p53 induced upregulation of Bax and Sp1 in ODN-treated p53-null HCT116 cells (Fig. 3B). The promoter activities of basal Sp1 (Sp1 binding element reporter) and Bax were also increased by the transfection of WT and C-terminal domain of p53 (Fig. 3C). These results showed that the C-terminal domain of p53 contributes to ODN-mediated Sp1 upregulation.

3.4. C-terminal domain of p53 interacts with and modulates Sp1 stability

Considering that the C-terminal domain of p53 induced Sp1 expression, we further characterized whether the C-terminal domain of p53 interacts with Sp1. We transfected each construct, performed Flag-antibody immunoprecipitation, and determined Sp1 level in p53-null HCT116 cells. The WT and C-terminal domain of p53 interacted with Sp1 (Fig. 4A). To investigate whether the C-terminal domain of p53 modulates Sp1 stability in a time-dependent manner, we treated the p53-null HCT116 cells with cycloheximide (CHX). The overexpression of the C-terminal domain of p53 markedly enhanced the half-life of Sp1 (Fig. 4B). Furthermore, the WT and C-terminal domain of p53 dramatically inhibited Sp1 ubiquitination, but the N-terminal domain mutant did not exhibit these effects (Fig. 4C). These data indicated that p53 induces Sp1 stabilization via the C-terminal domain.

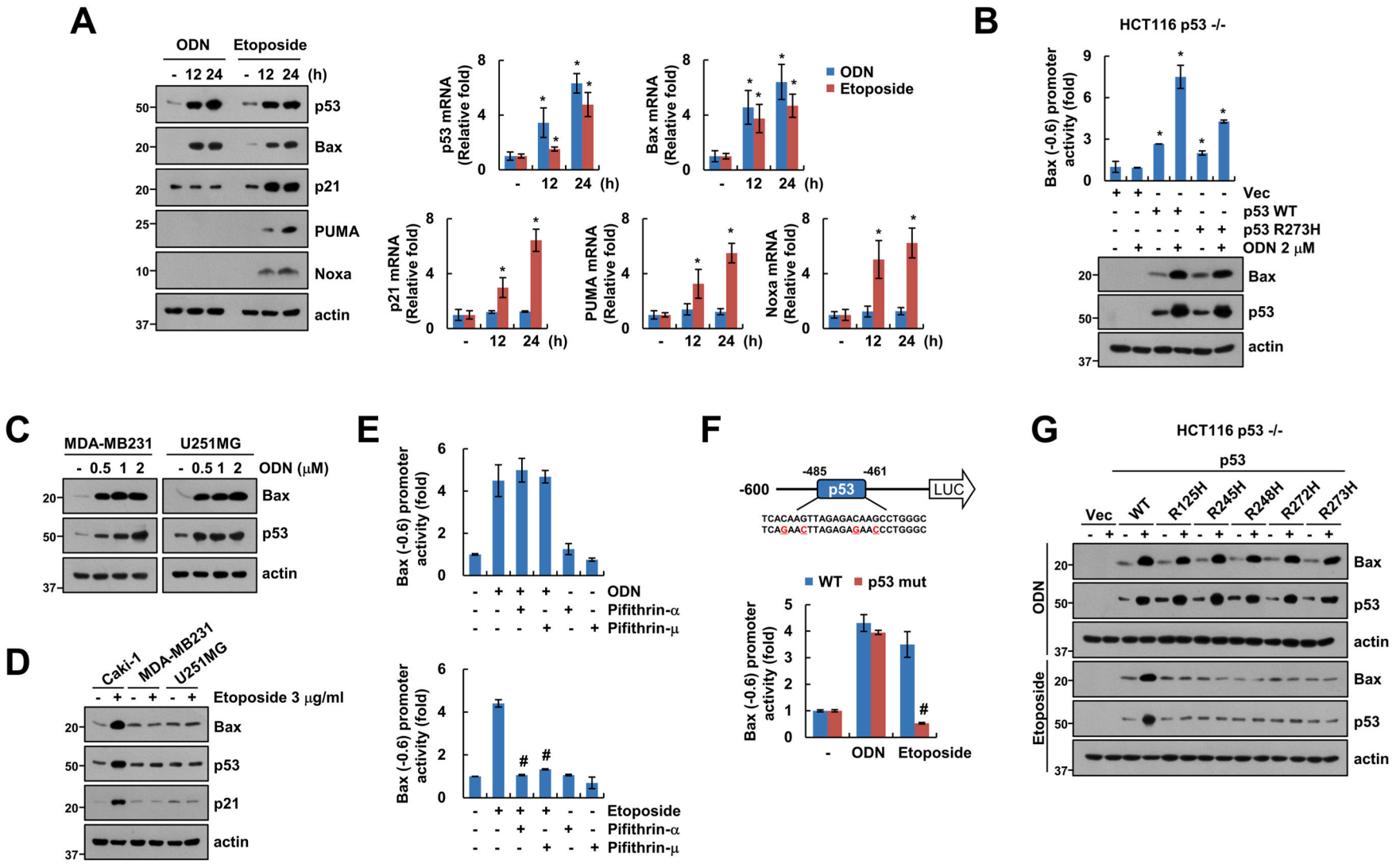

Fig. 1. Odanacatib (ODN) induces the transcriptional regulation of p53-independent Bax upregulation. (A) Caki-1 cells were treated with 2 μM ODN or 3 μg/mL etoposide for the indicated periods. **(B)** p53-null (−/−) HCT116 cells were transiently co-transfected with a vector, wild-type (WT) p53, or mutant p53 (R273H) with Bax/-600 promoter and then treated with 2 μM ODN for 12 h. The cells were lysed, and promoter activity and protein levels were measured. **(C, D)** Cancer cell lines were treated with 0.5–2 μM ODN (**C**) or 3 μg/mL etoposide (**D**) for 24 h. **(E)** Caki-1 cells were transiently transfected with Bax/-600 promoter. After the cells were pretreated with 5 μM pifithrin-α or 5 μM pifithrin-μ for 30 min, they were treated with 2 μM ODN or 3 μg/mL etoposide for 12 h. The cells were lysed, and the promoter activity was measured. **(F)** Caki-1 cells were transfected with Bax/-600 WT and p53-binding site mutant (p53 Mut) promoter and treated with 2 μM ODN for 12 h. The cells were lysed, and the promoter activity was measured. **(G)** p53-null (−/−) HCT116 cells were transiently transfected with WT and mutant p53 (R125H, R245H, R248H, R272H, and R273H) and then treated with 2 μM ODN or 3 μg/mL etoposide for 24 h. The protein and mRNA expression levels were determined using (**A**–**D** and **F**) western blotting and (**A**) qPCR, respectively. Values in the graphs (**A**, **B**, **E**, and **F**) represent the mean ± SD of three independent experiments. *$p < 0.01$ compared with the control. #$p <$ 0.01 compared with the etoposide.

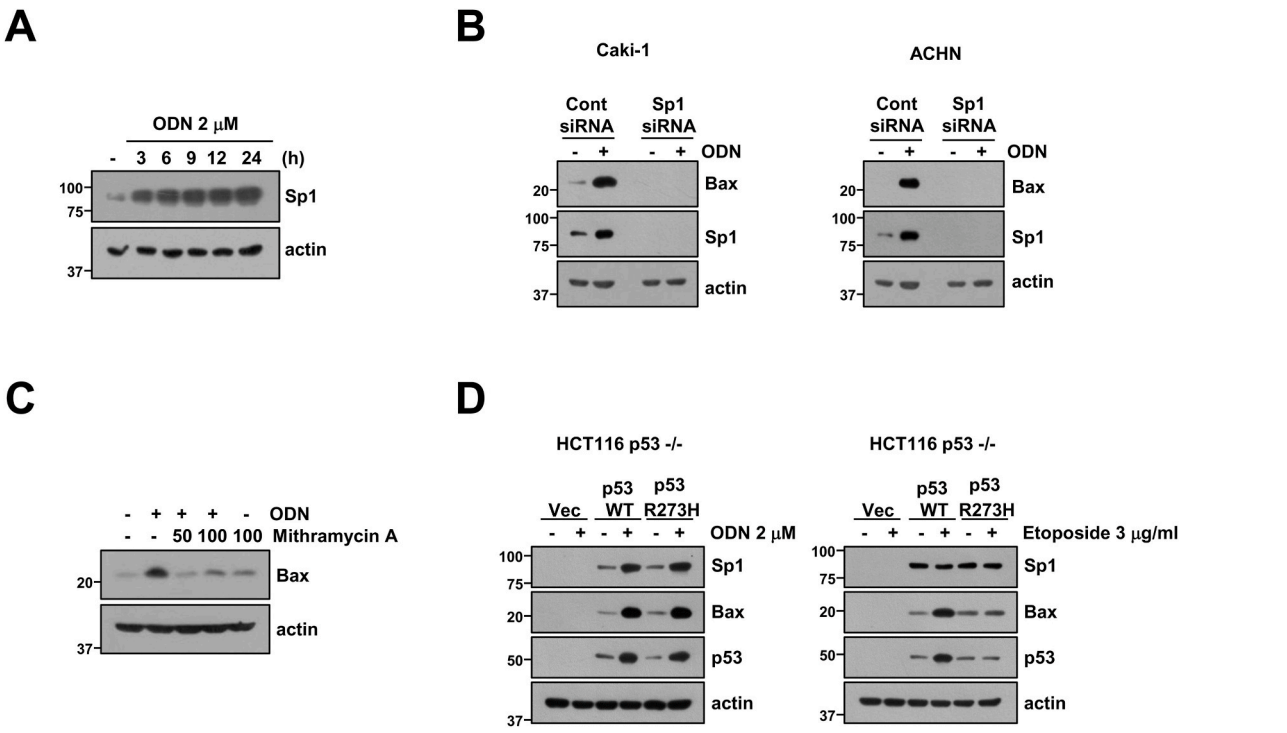

Fig. 2. Sp1 contributes to ODN-induced Bax upregulation in WT and mutant p53 cancer cells. (A) Caki-1 cells were treated with 2 μM ODN for the indicated periods. **(B)** Caki-1 and ACHN cells were transfected with control siRNA or Sp1 siRNA and treated with 2 μM ODN for 24 h. **(C)** Caki-1 cells were pretreated with 50–100 μM mithramycin A for 30 min and treated with 2 μM ODN for 24 h. **(D)** p53-null (−/−) HCT116 cells were transiently transfected with WT p53 and mutant p53 (R273H) and treated with 2 μM ODN or 3 μg/mL etoposide for 24 h. (**A**–**D**) Protein expression level was determined using western blotting.

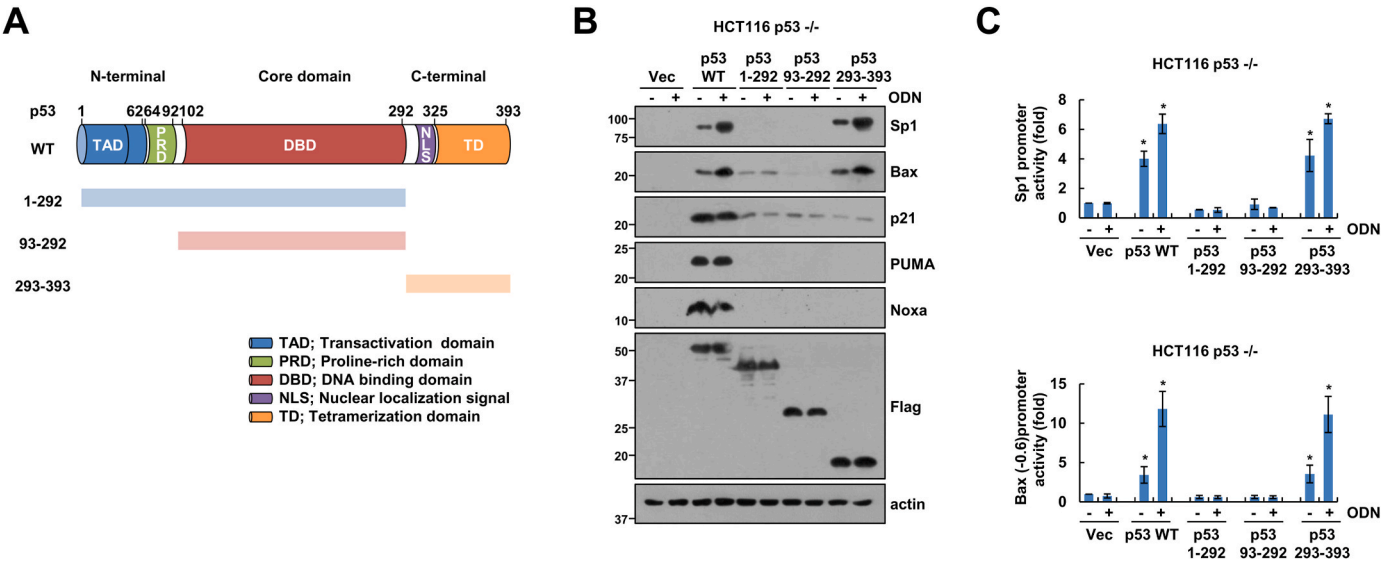

Fig. 3. C-terminal domain of p53 is involved in the ODN-mediated upregulation of Sp1 and Bax expression. (A) Overview of the N-terminal domain (1–292), DNA-binding core domain (93–292), and C-terminal domain (293–393) of WT p53 and its deletion mutants. **(B, C)** p53-null (−/−) HCT116 cells were transiently transfected with WT p53 and its deletion mutants and then treated with 2 μM ODN for 24 h. Protein expression level was determined using by western blotting (**B**). The promoter activities of Sp1 and Bax were determined (**C**). Values in the graphs (**C**) represent the mean ± SD of three independent experiments. *$p < 0.01$ compared with the control.

3.5. BAP1 is a C-terminal domain of p53-mediated Sp1 stabilizing deubiquitinating enzyme

To identify specific deubiquitinases (DUBs) that can stabilize Sp1, we have co-transfected 50 different siRNAs to knockdown 50 respective DUBs and the C-terminal domain of p53 in p53-null HCT116 cells. To examine the effect of DUBs on Sp1, C-terminal domain of p53, and protein level of Bax, we performed western blotting. Knockdown of seven DUBs (USP13, USP37, USP41, DUB3, OTUB1, OTUD7A, and BAP1) inhibited Sp1 upregulation by the C-terminal domain of p53-transfected cells. OTUB1, OTUD7A, and BAP1 downregulated Sp1 and Bax expression (Fig. 5). Because p53 downregulation did not induce Sp1-mediated Bax upregulation, we excluded OTUB1 and OTUD7A, as they induce the degradation of the C-terminal domain of p53. After

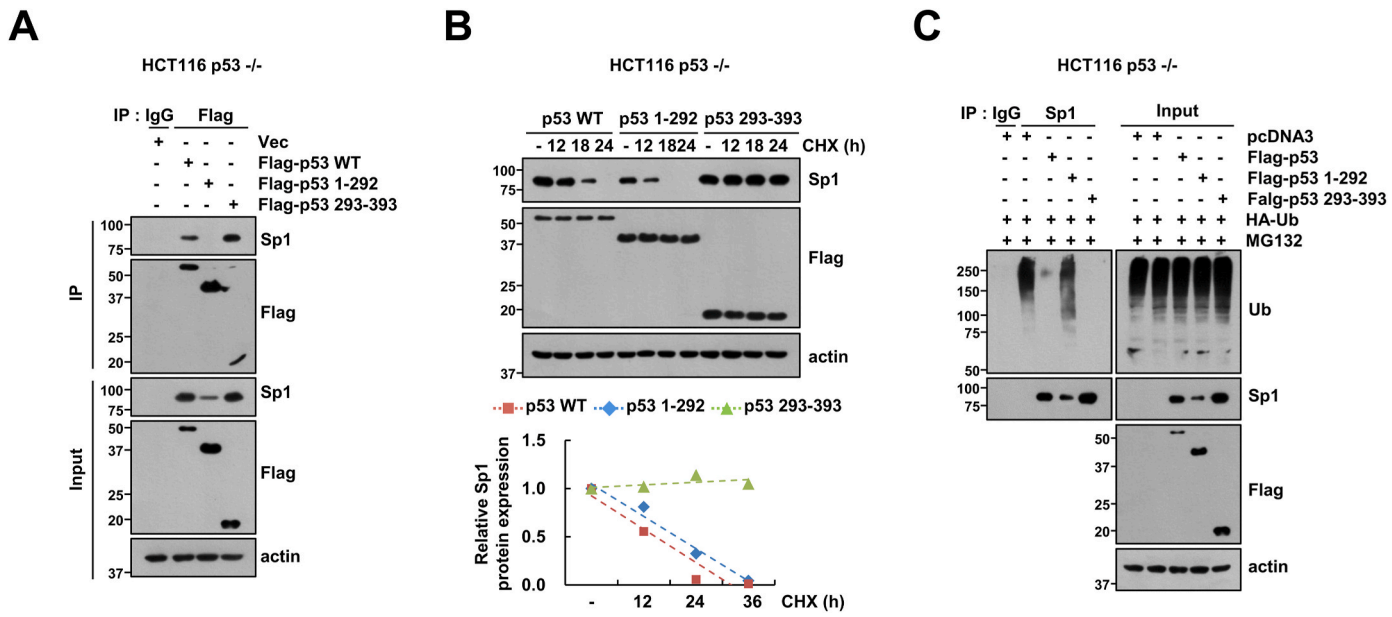

Fig. 4. C-terminal domain of p53 stabilizes Sp1. (A) p53-null (−/−) HCT116 cells were transfected with the vector, WT p53 or its deletion mutants. The interaction of WT p53 or its deletion mutants was demonstrated by immunoprecipitation (IP). **(B)** p53-null (−/−) HCT116 cells were transfected with WT p53 or its deletion mutants and treated with 20 μg/mL cycloheximide (CHX) for the indicated periods. **(C)** p53-null (−/−) HCT116 cells were co-transfected with the vector, WT p53, or its deletion mutants and HA-ubiquitin (HA-Ub) and then treated with 0.5 μM MG132 for 12 h to analyze Sp1 ubiquitination. IP was performed using an anti-Sp1 antibody. (**A**–**C**) Protein expression level was determined using western blotting.

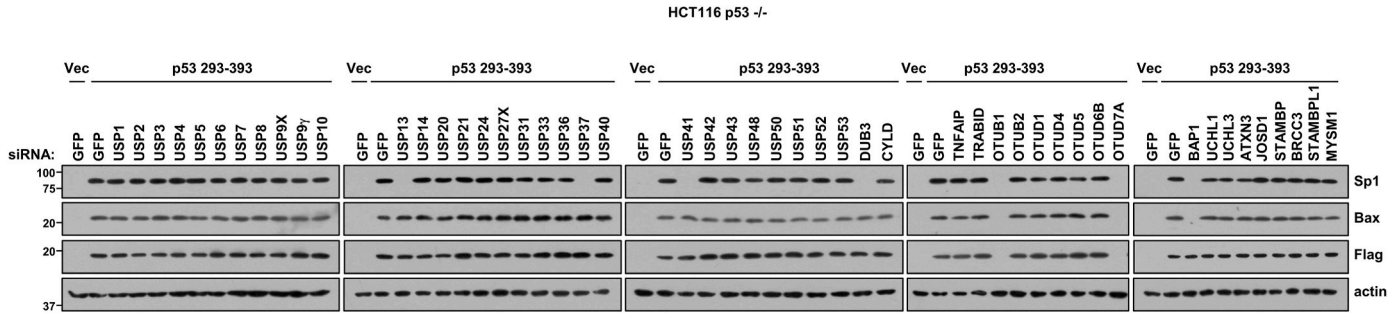

Fig. 5. Deubiquitinases participate in Sp1-dependent Bax regulation. p53-null (−/−) HCT116 cells were co-transfected with control siRNA or each DUB siRNA, together with C-terminal domain (293–393) of p53. Protein expression level was determined using western blotting.

verifying the interaction between DUBs and Sp1, we further confirmed whether BAP1 likely affects p53/Sp1 axis-mediated Bax upregulation in ODN-treated WT p53 Caki-1 cells. We also measured the alteration of ODN-induced p53, Sp1, and Bax upregulation after BAP1, OTUD7A, or OTUB1 siRNA treatment. Interestingly, the transfection of BAP1 siRNA, and not OTUD7A and OTUB1 siRNAs, still upregulated p53 expression in ODN-treated Caki-1 cells (Fig. 6A). To investigate the functional role of BAP1, we used an inactivating mutation (C91A) of BAP1. When the C-terminal domain of p53 was expressed in p53-null HCT116 cells, BAP1 C91A failed to upregulate Sp1 and Bax expression, indicating that the enzymatic activity of BAP1 is critical for Sp1 stability in ODN-treated cells (Fig. 6B). We also found similar results in WT p53 Caki-1 cells (Fig. 6C). Furthermore, to investigate the effect of BAP1 on the ubiquitination level of endogenous Sp1, we transfected WT and C91A BAP1 in Caki-1 cells. WT BAP1 reduced the ubiquitination levels of Sp1, whereas C91A BAP1 did not reduce ubiquitination levels (Fig. 6D). Therefore, these data suggested that ODN induces Sp1 stabilization, which is mediated by the C-terminal domain of p53 and is strongly linked to the BAP1.

3.6. ODN induces BAP1 interaction with Sp1

Next, we elucidated the molecular mechanisms underlying the BAP1-mediated stabilization of Sp1 during ODN treatment. We found that the protein levels of BAP1 were not altered by ODN treatment in Caki-1 cells (Fig. 6A). We postulated that ODN may influence the interaction between BAP1 and Sp1. To address this hypothesis, we performed an immunoprecipitation assay. Interestingly, ODN and cathepsin K siRNA treatment markedly increased Sp1 and BAP1 interaction (Fig. 7A). To investigate the functional role of p53, we tested the interaction between Sp1 and BAP1 after p53 immunoprecipitation in ODN- and cathepsin K siRNA-treated cells and identified more p53, Sp1, and BAP1 protein complexes in the ODN- and cathepsin K siRNA-treated cells (Fig. 7B). We also detected three protein complexes in the cells transfected with the WT and C-terminal domain of p53 in p53-null HCT116 cells treated with ODN and cathepsin K siRNA, but we could not identify complexes in vector-transfected cells (Figs. 7C and D). These data demonstrated that the C-terminal domain of p53 can effectively enhance Sp1 stability by increasing the interaction with BAP1 and Sp1.

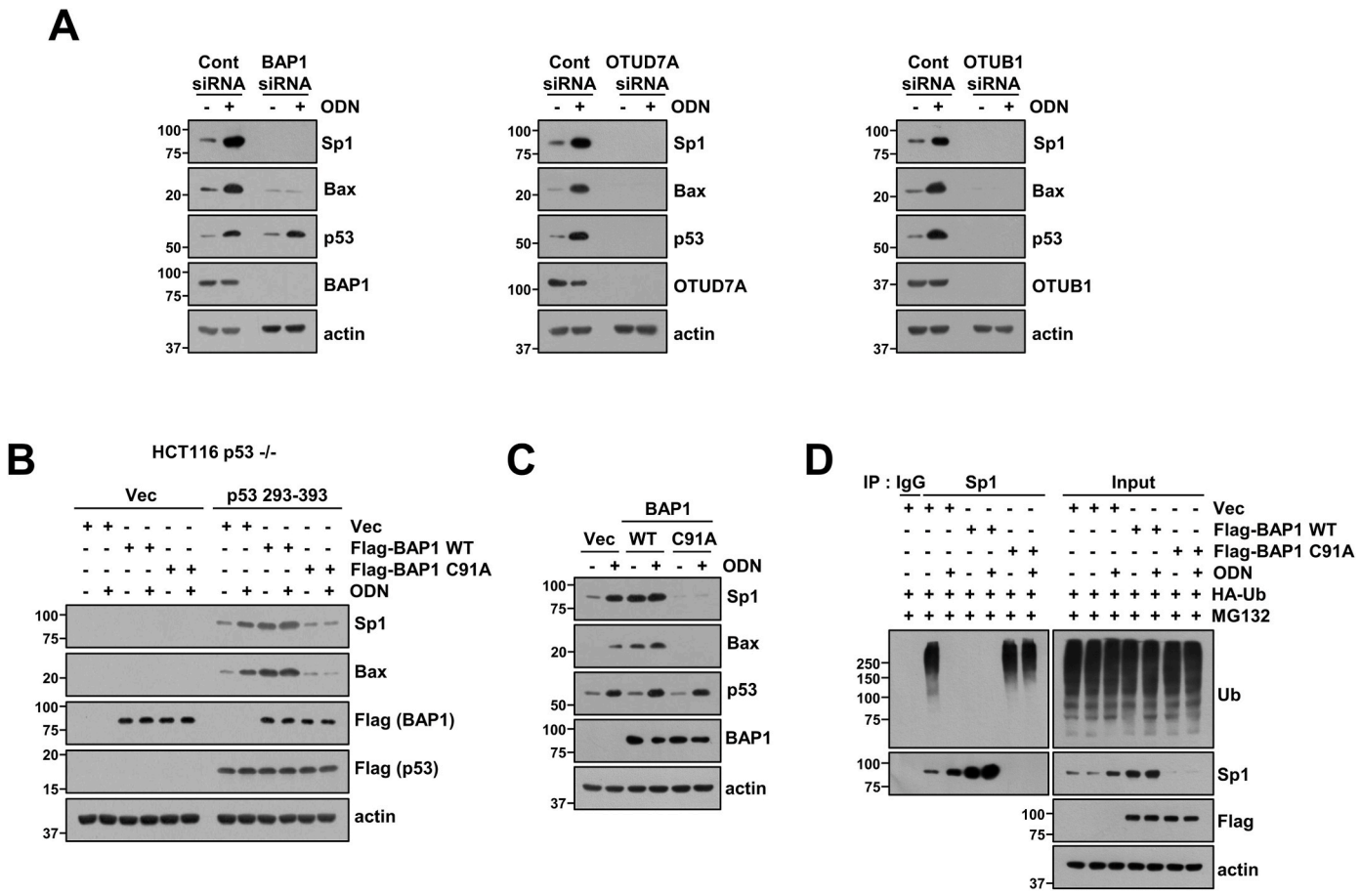

Fig. 6. BAP1 decreases Sp1 ubiquitination by the C-terminal domain of p53. (A) Caki-1 cells were transfected with control siRNA or 3 DUB (BAP1, OTUD7A, and OTUB1) siRNAs and treated with 2 μM ODN for 24 h. **(B)** p53-null (−/−) HCT116 cells were co-transfected with the vector or p53 deletion mutant (293–393), together with WT BAP or BAP mutant (C91A), and treated with 2 μM ODN for 24 h. **(C)** Caki-1 cells were transfected with the vector, WT BAP, or BAP mutant (C91A) and treated with 2 μM ODN for 24 h. **(D)** Caki-1 cells were co-transfected with the vector, WT BAP, or BAP mutant (C91A) and HA-ubiquitin (HA-Ub), and treated with 0.5 μM MG132 for 12 h to analyze Sp1 ubiquitination. Immunoprecipitation was performed using an anti-Sp1 antibody. (**A–D**) Protein expression level was determined using western blotting.

3.7. ODN induces Bax upregulation via BAP1 phosphorylation

We investigated whether ODN modulates BAP1 phosphorylation. After conducting immunoprecipitation with BAP1 antibody, we determined the phosphorylation of Ser/Thr or Tyr residue using a specific phospho-antibody (Fig. 8A). ODN treatment induced the phosphorylation of BAP1 at Ser 592 residue in a time-dependent manner (Fig. 8B). To investigate the functional role of Ser 592 phosphorylation in BAP1, we used the BAP1 mutant (S592A). S592A BAP1 failed to upregulate Sp1 and Bax expression, indicating that the phosphorylation of BAP1 at Ser 592 is crucial for Sp1 stability in ODN-treated cells (Fig. 8C). Furthermore, ODN treatment increased protein interaction between phopho-BAP1 and Sp1 (Fig. 8D). By using immunofluorescence staining, we confirmed that phospho-BAP1 colocalized with Sp1 in the nucleus in ODN-treated Caki-1 cells (Fig. 8E). However, green fluorescence of phopho-BAP1did not detect in ODN-untreated cells. To verify the interaction with BAP1 and Sp1, we performed the proximity ligation assay. Sp1-BAP1 interaction was increased by ODN treatment (Fig. 8F). These findings indicated that cathepsin K inhibition increases Sp1 stabilization via BAP1 Ser 592 phosphorylation.

3.8. Mitochondrial ROS production is critical for ODN-mediated DNA damage and BAP1 phosphorylation

We previously reported that ODN and cathepsin K siRNA generate mitochondrial ROS through Raptor degradation [9,10]. To confirm the *in vivo* protective effects of mitochondrial ROS scavenger Mito-TEMPO against ODN-induced mitochondrial ROS generation, we performed DCF-DA or MitoSOX staining in a zebrafish model for visualization. ODN treatment markedly generated a fluorescence signal in zebrafish larvae (Fig. 9A), suggesting that mitochondrial ROS was generated in the presence of ODN. Pretreatment with Mito-TEMPO or NAC reduced the ODN-induced increase in mitochondrial ROS production (Fig. 9A). To examine whether Mito-TEMPO could prevent ODN-induced DNA damage, we performed the comet assay, a sensitive method to assess DNA strand breaks in cells. We did not detect a comet tail moment in vehicle-, NAC-, and Mito-TEMPO alone-treated cells, whereas ODN markedly enhanced DNA migration. Mito-TEMPO or NAC markedly decreased ODN-induced DNA migration (Fig. 9B). The DNA damage blocking effect of Mito-TEMPO was also confirmed by analyzing the phosphorylation status of γH2AX and 8-OHdG. Pretreatment with Mito-TEMPO or NAC could effectively prevent ODN-induced γH2AX phosphorylation and significantly suppressed 8-OHdG production (Fig. 9C). Next, we investigated the role of mitochondrial ROS in ODN-mediated BAP1/Sp1/Bax axis. Interestingly, the Mito-TEMPO and NAC markedly inhibited ODN- and cathepsin K siRNA-induced BAP1 phosphorylation and Sp1 and Bax upregulation (Fig. 9D). Proteomic analysis has revealed that BAP1 is a substrate of DNA damage response kinases [22]. Consistently, our findings showed that an ATM inhibitor (KU-55933) and a DNA-PKcs inhibitor (NU7441) markedly inhibited ODN- and cathepsin K siRNA-induced BAP1 phosphorylation and Sp1 and Bax upregulation (Fig. 9E). These results suggested that BAP1 is phosphorylated after DNA

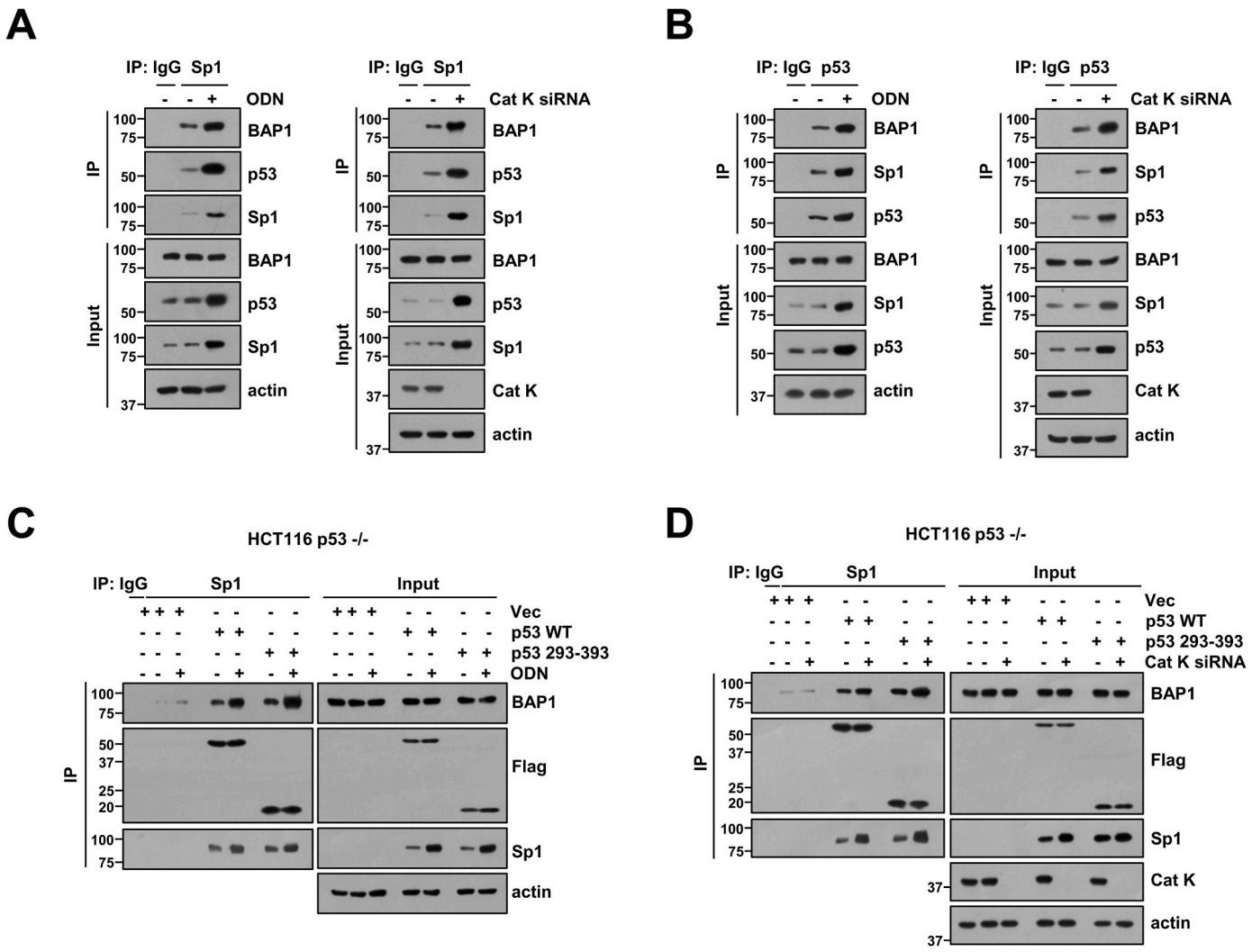

Fig. 7. ODN interacts with Sp1 and BAP1. (A, B) Caki-1 cells were treated with 2 μM ODN or Cat K siRNA for 24 h. Endogenous protein-protein interaction was demonstrated by IP using anti-Sp1 **(A)** or anti-p53 **(B)** antibodies, respectively. **(C)** p53-null (−/−) HCT116 cells were transfected with the vector, WT p53, or p53 deletion mutant (293–393) and treated with 2 μM ODN for 24 h. **(D)** p53-null (−/−) HCT116 cells were co-transfected with the vector, WT p53, or p53 deletion mutant (293–393) and Cat K siRNA. (**A–D**) Protein expression level was determined using western blotting.

damage in a mitochondrial ROS-dependent manner.

3.9. Knockdown of BAP1 inhibits ODN plus oxaliplatin-induced apoptosis

We examined the effect of BAP1 on apoptosis induced by the combined treatment of ODN and oxaliplatin. The combined treatment markedly increased the sub-G1 population, promoted PARP cleavage, and upregulated Sp1 and Bax expression in WT p53 Caki-1 cells. However, siRNA-knocked down BAP1 markedly inhibited the ODN and oxaliplatin-induced apoptosis and upregulation of Sp1 and Bax (Fig. 10A). Furthermore, we observed that the combined treatment of ODN plus oxaliplatin/etoposide induced low colony formation, cell death, and upregulation of Sp1 and Bax expression in the WT and C-terminal domain mutant of p53-transfected p53-null HCT116 cells; however, this was not observed in the vector-transfected p53-null HCT116 cells (Figs. 10B and C). To further confirm the effect of S592A BAP1 on the combined treatment-induced apoptosis, we transfected WT and S592A BAP1 in Caki-1 cells. The ectopic expression of S592A BAP1 completely inhibited the combined treatment-induced apoptosis (Fig. 10D). Furthermore, pretreatment with PI3K/AKT inhibitors (wortmannin and LY294002), mitochondrial ROS scavenger (NAC and Mito-TEMPO), ATM inhibitor (KU-55933), and DNA-PKcs inhibitor (NU7441) significantly inhibited apoptosis induced by the combined treatment of ODN plus oxaliplatin (Fig. 10E). These results suggested that ODN plus oxaliplatin-induced apoptosis is caused by Bax upregulation, which is modulated by Sp1 stabilization via BAP1 activation that is dependent on the C-terminal domain of p53.

4. Discussion

In this study, we demonstrated that ODN upregulated Bax expression and enhanced oxaliplatin-induced apoptosis in cancer cells. ODN-induced Bax upregulation was regulated by Sp1 stabilization, which was modulated by BAP1-dependent deubiquitination mediated by the C-terminal domain of p53. ODN induced the phosphorylation of BAP1 at Ser 592 and enhanced the interaction of Sp1 and BAP1, resulting in Sp1 deubiquitination and destabilization. Interestingly, ODN-mediated mitochondrial ROS production induced BAP1 phosphorylation, DNA damage, and Bax upregulation. Therefore, ODN enhanced oxaliplatin-induced apoptosis by interacting with BAP1 and Sp1 to induce Sp1 stabilization-mediated Bax upregulation (Fig. 11).

Most mutated sites of p53 are located in the DNA-binding domain of p53. Since mutant p53 have gain-of-function leading to the induction tumor growth, invasion, and resistance to diverse anticancer drugs.

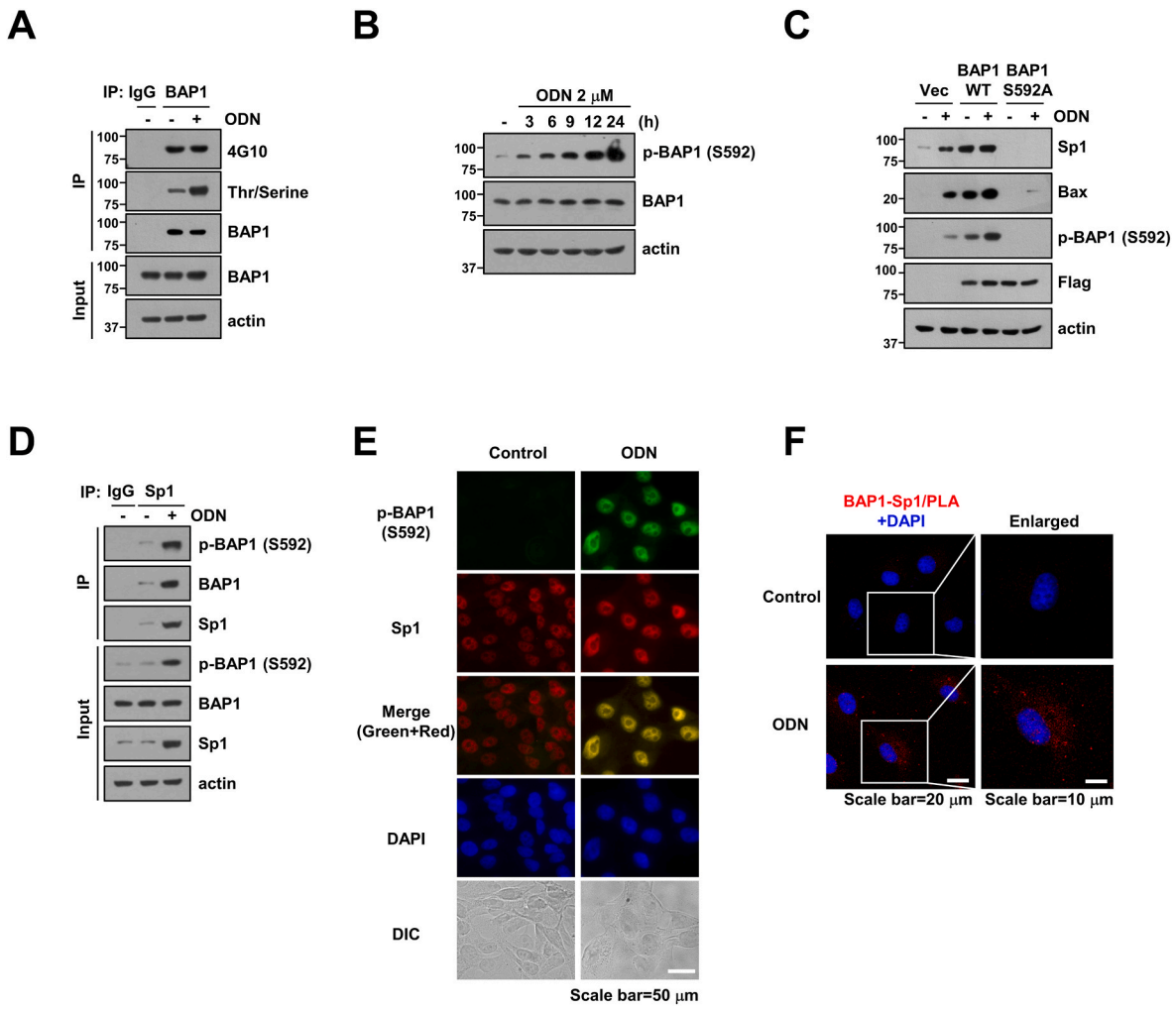

Fig. 8. ODN phosphorylates BAP1 at Ser 592. (A) Caki-1 cells were treated with 2 μM ODN for 24 h. Endogenous protein-protein interaction was demonstrated by IP. **(B)** Caki-1 cells were treated with 2 μM ODN for the indicated periods. **(C)** Caki-1 cells were transfected with vector, WT BAP1, or mutant BAP1 (S592A) and treated with 2 μM ODN for 24 h. **(D)** Caki-1 cells were treated with 2 μM ODN for 24 h. Endogenous protein-protein interaction was demonstrated by IP. **(E, F)** Caki-1 cells were treated with 2 μM ODN for 24 h. After treatment, cells were fixed and subjected to immunocytochemistry for phospho-BAP1 (green), Sp1 (red), and DAPI (blue) (**E**). Proximity Ligation Assay (PLA) was performed for interaction between BAP1 and Sp1. PLA signal is red (**F**). (**A**–**D**) Protein expression level was determined using western blotting. (For interpretation of the references to colour in this figure legend, the reader is referred to the Web version of this article.)

Especially R273H of mutant p53 activates transcription genes of DNA replication and cell cycle [23,24], and increases proliferation and metastasis of cancer cells [25]. Previously, cathepsin K deficiency induces p53-dependent Bax upregulation [10]. We found that the ectopic expression of the p53 mutant (R273H), i.e., the DNA-binding CD of p53, also induced Bax upregulation in ODN-treated p53-null HCT116 cells (Fig. 1F). The p53 mutant could have been formed due to ODN because several p53 mutant-reactivating compounds, such as alkylators, potentially bind to thiol groups in the p53 mutant and stimulate refolding of the mutant protein [26,27]. ODN cannot reactivate mutant p53. Therefore, among the expressed p53 target proteins, only Bax showed an increased expression after ODN treatment. In addition, ODN-induced Bax promoter activity was not inhibited by pifithrin-α and pifithrin-μ (Fig. 1E). p53 contains four different functional domains, namely N-terminal transactivation domain (residues 1–93), DNA-binding CD (residues 93–292), tetramerization domain (TET residues 325–355), and C-terminal negative regulatory domain (NRD residues 367–393) [28]. We generated a deletion mutant (residues 293–393) of p53 that contained the TET and C-terminal NRD (Fig. 3A). The S100 protein, a small EF-hand calcium-binding protein, interacts with C-terminal TET and NRD of p53 [29]. Interaction between S100 and C-terminal TET and NRD of p53 helps stimulate or inhibit p53 transcriptional activity [30,31]. The 14-3-3 family proteins also bind to C-terminal TET and NRD of p53 and affect p53 transcriptional activity [32]. The phosphorylation of p53 at Ser 392 enhances tetramer formation and stabilization [33]. TET mutation reduces p53 transcriptional activity [34]. Several proteins have been reported to modulate p53 oligomerization in vitro [35]. Protein–protein interactions are critical for the identification of novel p53 functions. Our results demonstrated that the C-terminal domain of p53 (residues 293–393) physically interacted with Sp1 and enhanced Sp1 stability (Fig. 4A and B). Therefore, the modulatory mechanism of the C-terminal domain of p53 (residues 293–393) in Sp1 stabilization should be further investigated in detail.

p53 and Sp1 bind to similar consensus sequences at the GC boxes of the Bax promoter region, suggesting that both transcription factors may interplay in transcriptional regulation. Li et al. [20] performed genome-wide shRNA screening and ChIP-seq and demonstrated Sp1 as a central regulator of p53-mediated apoptosis. Sp1 depletion by shRNA and Sp1 ectopic expression mainly affect about half of the p53 target genes [20]. The knockdown of p15, a PCNA-associated factor, promotes the interaction between p53 and Sp1, thereby inhibiting cell proliferation [36]. The functional activity of Sp1 is determined by expression levels, post-translational modification, and interactions with other proteins. Post-translational Sp1 modifications, such as glycosylation,

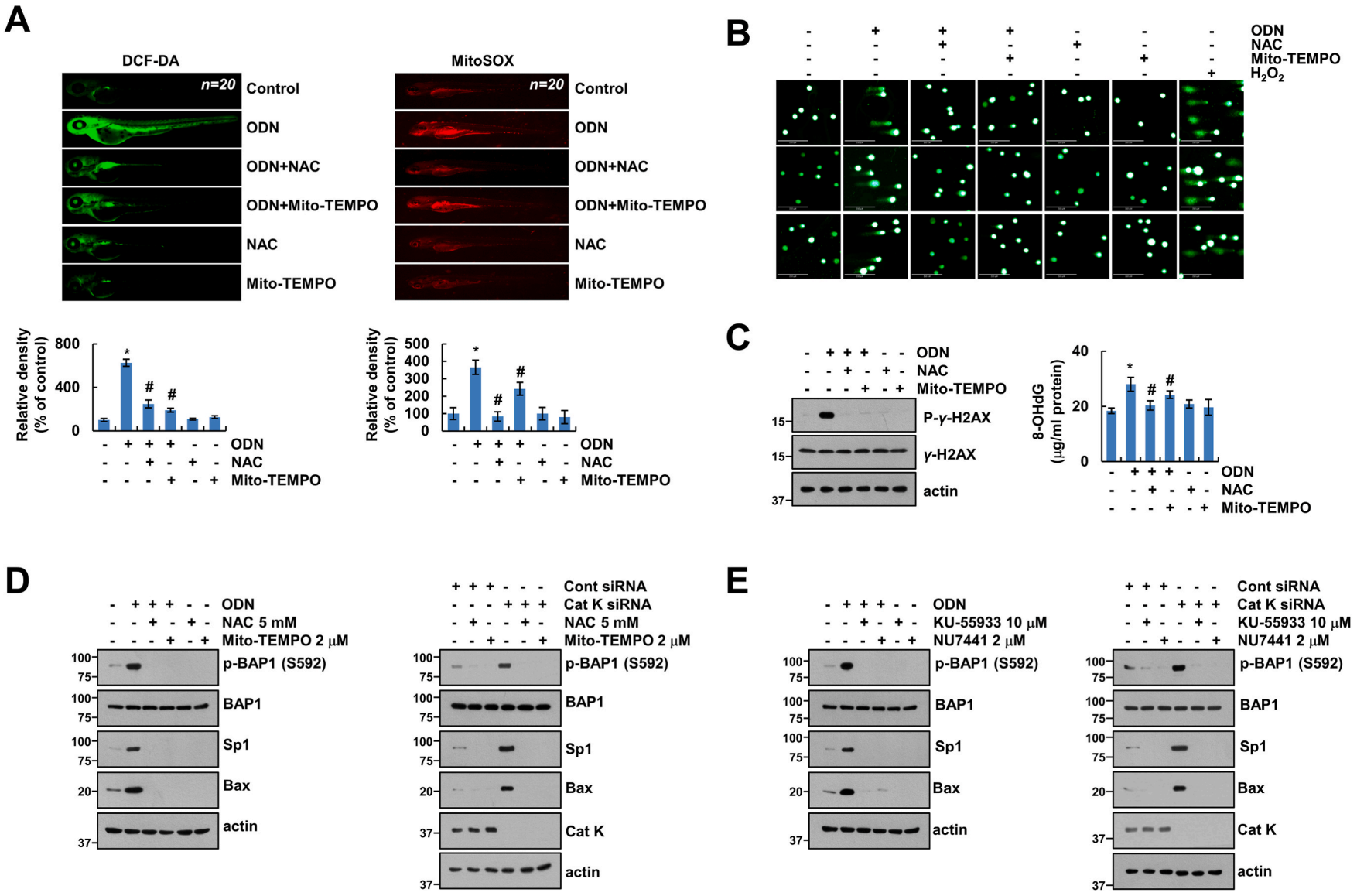

Fig. 9. ODN-induced mitochondrial ROS generation is involved in BAP1/Sp1/Bax activation. (A) Zebrafish larvae or (**B, C**) Caki-1 cells were pretreated with ROS scavengers (5 mM NAC and 2 μM Mito-TEMPO) for 1 h and then treated with 2 μM ODN for 24 h. ROS levels were observed under a fluorescence microscope after DCF-DA or MitoSOX staining (**A**). Representative images of the comet assay results were captured using a fluorescence microscope (× 200) (**B**). p-γH2AX level was measured by western blotting, and the 8-OHdG level of the DNA samples of the cells was assessed **(C). (D)** Caki-1 cells were pretreated with ROS scavengers (5 mM NAC and 2 μM Mito-TEMPO) and then treated with 2 μM ODN or Cat K siRNA for 24 h. **(E)** Caki-1 cells were pretreated with 10 μM KU-55933 or 2 μM NU7441 and then treated with 2 μM ODN or Cat K siRNA for 24 h. (**C**–**E**) Protein expression level was determined using western blotting. Values in the graphs (**A, C**) represent the mean ± SD of three independent experiments. *$p < 0.01$ compared with control. #$p < 0.01$ compared with ODN treatment.

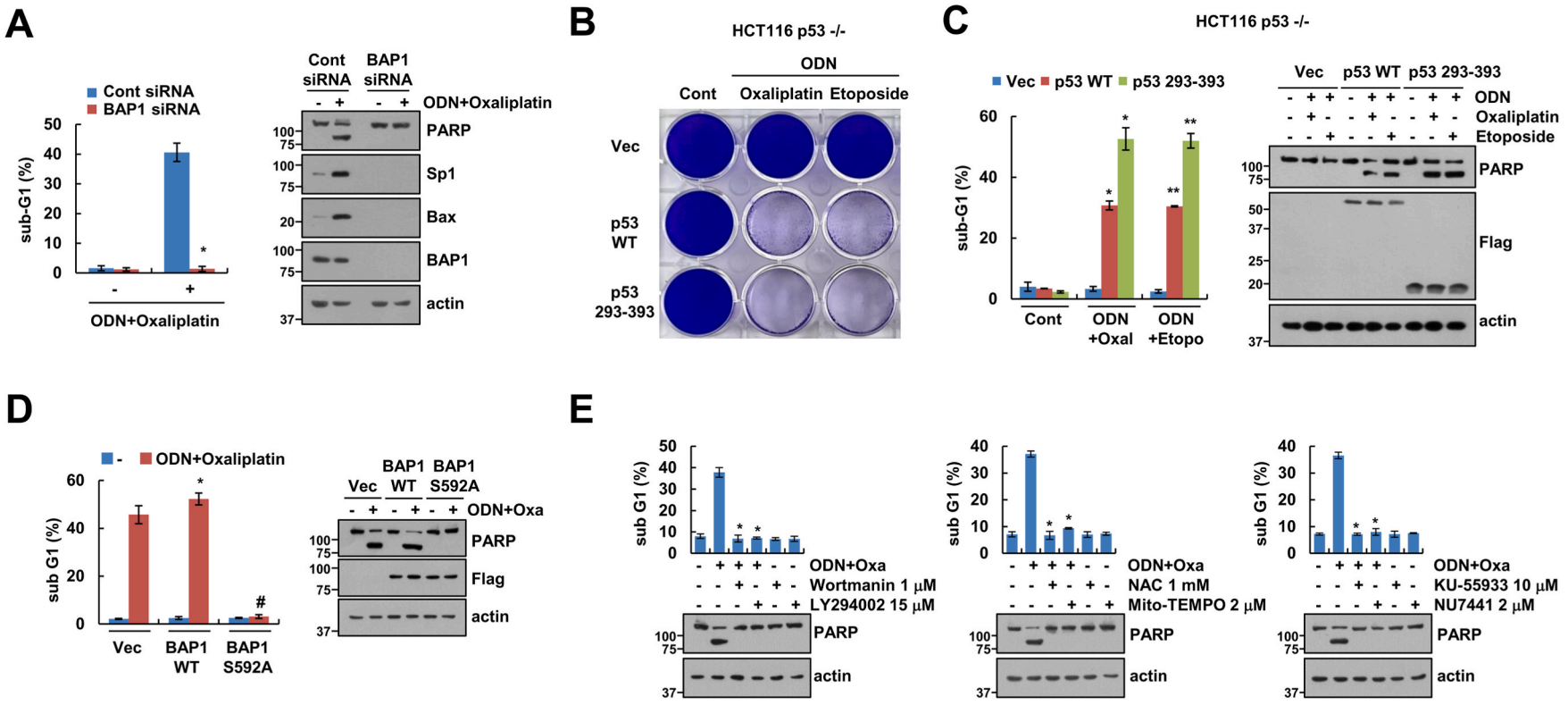

Fig. 10. Effect of BAP1 on ODN plus oxaliplatin-induced cancer cell death. (A) Caki-1 cells were transfected with control siRNA or BAP1 siRNA and treated with a combination of 2 μM ODN and 25 μM oxaliplatin for 24 h. **(B, C)** p53-null (−/−) HCT116 cells were transfected with the vector, WT p53, or p53 deletion mutant (293–393) and treated with a combination of 2 μM ODN and 25 μM oxaliplatin/3 μg/mL etoposide for 24 h. Colony formation was measured using crystal violet staining. **(D)** Caki-1 cells were transfected with vector, WT BAP1, or BAP1 mutant (S592A) and treated with a combination of 2 μM ODN and 25 μM oxaliplatin for 24 h. **(E)** Caki-1 cells were pretreated with various inhibitors (1 μM wortmarnin, 15 μM LY294002, 5 mM NAC, 2 μM Mito-TEMPO, 10 μM KU-55933, or 2 μM NU7441) and treated with a combination of 2 μM ODN and 25 μM oxaliplatin for 24 h. Apoptosis and protein expression levels were measured using flow cytometry (**A**, **C**–**D**) and western blotting (**A**, **C**–**E**). Values in the graphs (**A**, **C**–**E**) represent the mean ± SD of three independent experiments. $*p < 0.01$ compared with ODN plus oxaliplatin in the vector. $**p < 0.01$ compared with ODN plus etoposide in the vector. $\#p < 0.01$ compared with ODN plus oxaliplatin in WT BAP1-transfected cells. (For interpretation of the references to colour in this figure legend, the reader is referred to the Web version of this article.)

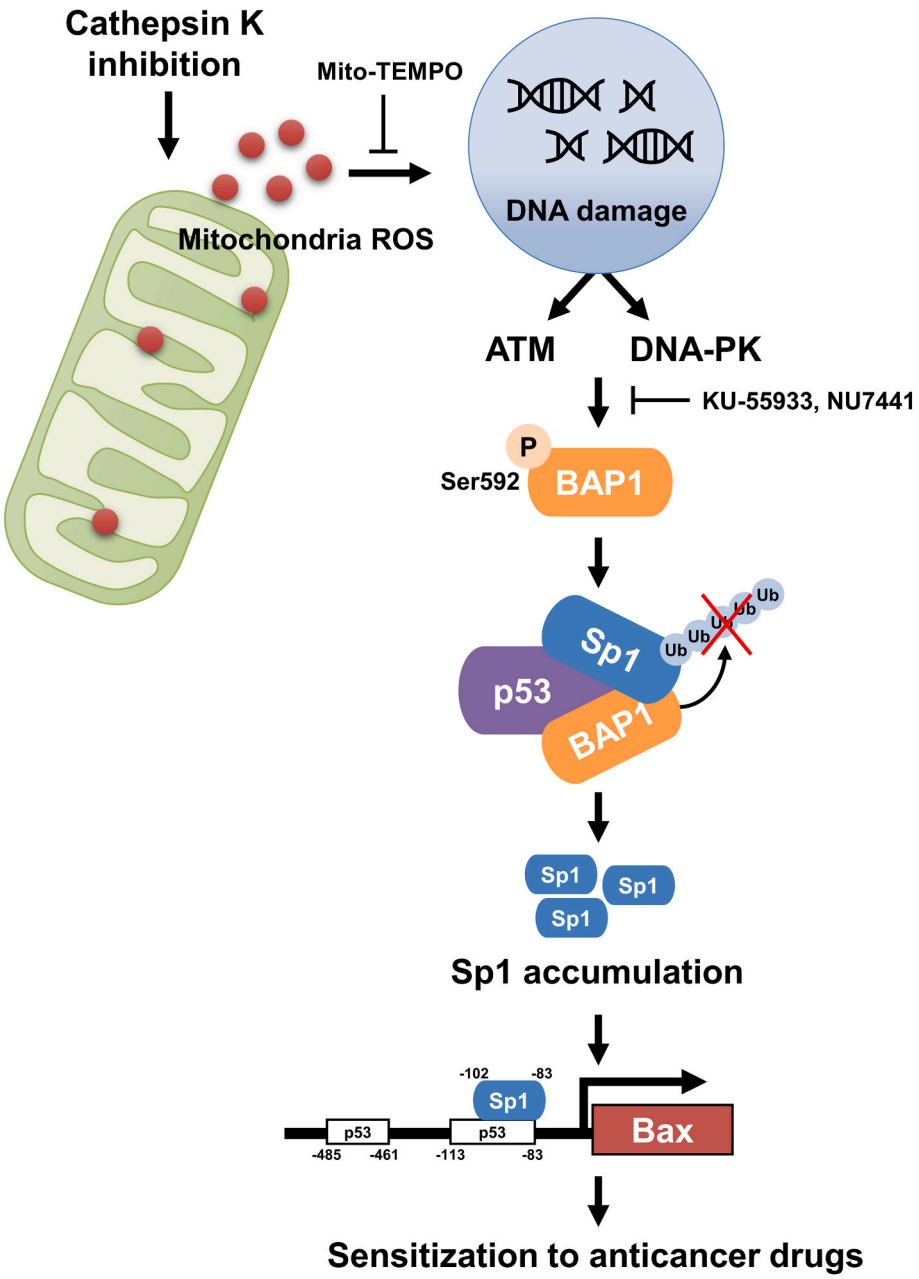

Fig. 11. Scheme of the mechanism of ODN-mediated Sp1 stabilization through mitochondrial ROS-dependent BAP1 activation.

phosphorylation, acetylation, sumoylation, and ubiquitination, regulate transcriptional activity and modulate target gene expression [37]. USP33 directly deubiquitinates Sp1, stabilizing Sp1 expression and contributing to invasion and metastasis through c-Met upregulation in hepatocellular carcinoma [38]. Unfortunately, we did not detect a decrease in Sp1 expression in the USP33 siRNA experiment (Fig. 5), which could be because of difference in cell line and p53 C-terminal domain expression conditions.

BAP1 belongs to the DUB superfamily of enzymes that contain the ubiquitin C-terminal hydrolase (UCH) domain. BAP1 exhibits multiple functions, including transcription regulation, DNA repair, and replication, through the coordination of chromatin structures and functions [39]. Previous studies showed that BAP1 plays a role in cell death [39,40]. BAP1 induces apoptosis by releasing Bax through 14-3-3 protein interaction regardless of DUB activity [41]. BAP1 stabilizes type 3 inositol-1,4,5-triphosphate receptor, promoting Ca^{2+} release from the endoplasmic reticulum (ER) [42]. Excessive Ca^{2+} release from the ER is absorbed by the mitochondria, which induces cytochrome *c* release and cell death [43]. In this study, we found that BAP1 could stabilize Sp1, which led to the transcriptional activation of Bax in ODN-treated cells. In addition, the ectopic expression of BAP1 greatly decreased the ubiquitination level of Sp1 and the upregulation of Sp1 and Bax, whereas the catalytic mutant of BAP1 showed no apparent effect (Fig. 6B–D). In the presence of DNA damage, PI3K-related kinases (ATM, ATR, and DNA-PKcs) phosphorylate BAP1 at Ser 592 to increase its recruitment on the site of DNA damage and facilitate proper DNA repair [44,45]. Interestingly, the protein expression of BAP1 did not change, but Ser 592 phosphorylation increased with ODN treatment in a time-dependent manner (Fig. 8B). ODN caused mitochondrial ROS generation and DNA damage, which was inhibited by mitochondrial ROS scavenger pretreatment (Fig. 9A–C). Mito-TEMPO pretreatment inhibited ODN-induced BAP1 phosphorylation, increased Bax expression, and promoted apoptosis induced by the combined treatment of ODN and oxaliplatin (Figs. 9D and 10E).

5. Conclusion

Our findings suggested that ODN enhanced oxaliplatin-induced apoptosis by upregulating Bax. The ODN-induced upregulation of Bax expression was independent of p53 transcriptional activity. The C-terminal domain of p53 (residues 293–393) induced Sp1 stabilization strongly linked to BAP1 Ser 592 phosphorylation. Moreover, ODN-induced mitochondrial ROS generation was involved in DNA damage, BAP1 phosphorylation, upregulation of Sp1 and Bax, sensitization of anti-cancer drug-mediated apoptosis. Therefore, BAP1 was involved in ODN-mediated Sp1 stabilization and might be a potential target for cancer therapy in drug development.

Funding

This work was supported by an NRF grant funded by the Korea Government (MSIP) [NRF-2021R1A4A1029238, NRF-2019R1A2C2005921, and NRF-2020R1C1C1009889].

Author contributions

S.U.S., S.M.W., and T.K.K. conceived and designed the project; S.U.S., S.M.W., S.G.L., M.Y.K., and T.K.K. performed experiments and/or conducted data acquisition and analyses; H.S.L, Y.H.C., S.H.K., Y.C., K.M., and T.K.K. contributed technical/reagent materials, analytic tools, and/or grant support; S.U.S, S.M.W., H.S.L, Y.H.C., S.H.K., Y.C., and T.K.K. prepared, wrote, reviewed, and/or revised the manuscript. All authors discussed the results and commented on the manuscript. The authors read and approved the final manuscript.

Declaration of interests

The authors declare no conflict of interest.
Supplementary data to this article can be found online at.

Appendix A. Supplementary data

Supplementary data to this article can be found online at https://doi.org/10.1016/j.redox.2022.102336.

References

[1] R. Dai, Z. Wu, H.Y. Chu, J. Lu, A. Lyu, J. Liu, G. Zhang, Cathepsin K: the action in and beyond bone, Front. Cell Dev. Biol. 8 (2020) 433, https://doi.org/10.3389/fcell.2020.00433.
[2] F.K. Leusink, E. Koudounarakis, M.H. Frank, R. Koole, P.J. van Diest, S.M. Willems, Cathepsin K associates with lymph node metastasis and poor prognosis in oral squamous cell carcinoma, BMC Cancer 18 (2018) 385, https://doi.org/10.1186/s12885-018-4315-8.
[3] U. Verbovsek, C.J. Van Noorden, T.T. Lah, Complexity of cancer protease biology: cathepsin K expression and function in cancer progression, Semin. Cancer Biol. 35 (2015) 71–84, https://doi.org/10.1016/j.semcancer.2015.08.010.
[4] K. Garber, Two pioneering osteoporosis drugs finally approach approval, Nat. Rev. Drug Discov. 15 (2016) 445–446, https://doi.org/10.1038/nrd.2016.132.
[5] B.R. Troen, The regulation of cathepsin K gene expression, Ann. N. Y. Acad. Sci. 1068 (2006) 165–172, https://doi.org/10.1196/annals.1346.018.
[6] H.G. Bone, D.W. Dempster, J.A. Eisman, S.L. Greenspan, M.R. McClung, T. Nakamura, S. Papapoulos, W.J. Shih, A. Rybak-Feiglin, A.C. Santora, N. Verbruggen, A.T. Leung, A. Lombardi, Odanacatib for the treatment of postmenopausal osteoporosis: development history and design and participant characteristics of LOFT, the Long-Term Odanacatib Fracture Trial, Osteoporos. Int. 26 (2015) 699–712, https://doi.org/10.1007/s00198-014-2944-6.
[7] Y. Vashum, R. Premsingh, A. Kottaiswamy, M. Soma, A. Padmanaban, P. Kalaiselvan, S. Samuel, Inhibitory effect of cathepsin K inhibitor (ODN-MK-0822) on invasion, migration and adhesion of human breast cancer cells in vitro, Mol. Biol. Rep. 48 (2021) 105–116, https://doi.org/10.1007/s11033-020-05951-0.
[8] Q. Dai, F. Xie, Y. Han, X. Ma, S. Zhou, L. Jiang, W. Zou, J. Wang, Inactivation of regulatory-associated protein of mTOR (Raptor)/Mammalian target of rapamycin complex 1 (mTORC1) signaling in osteoclasts increases bone mass by inhibiting osteoclast differentiation in mice, J. Biol. Chem. 292 (2017) 196–204, https://doi.org/10.1074/jbc.M116.764761.
[9] S.U. Seo, S.M. Woo, M.W. Kim, H.S. Lee, S.H. Kim, S.C. Kang, E.W. Lee, K.J. Min, T. K. Kwon, Cathepsin K inhibition-induced mitochondrial ROS enhances sensitivity of cancer cells to anti-cancer drugs through USP27x-mediated Bim protein stabilization, Redox Biol. 30 (2020) 101422, https://doi.org/10.1016/j.redox.2019.101422.
[10] S.U. Seo, S.M. Woo, S. Kim, J.W. Park, H.S. Lee, Y.S. Bae, S.H. Kim, S.S. Im, J. H. Seo, K.J. Min, T.K. Kwon, Inhibition of cathepsin K sensitizes oxaliplatin-induced apoptotic cell death by Bax upregulation through OTUB1-mediated p53 stabilization in vitro and in vivo, Oncogene 41 (2022) 550–559, https://doi.org/10.1038/s41388-021-02088-7.
[11] T. Miyashita, J.C. Reed, Tumor suppressor p53 is a direct transcriptional activator of the human bax gene, Cell 80 (1995) 293–299, https://doi.org/10.1016/0092-8674(95)90412-3.
[12] E.C. Thornborrow, J.J. Manfredi, The tumor suppressor protein p53 requires a cofactor to activate transcriptionally the human BAX promoter, J. Biol. Chem. 276 (2001) 15598–15608, https://doi.org/10.1074/jbc.M011643200.
[13] R. Cianfrocca, M. Muscolini, V. Marzano, A. Annibaldi, B. Marinari, M. Levrero, A. Costanzo, L. Tuosto, RelA/NF-kappaB recruitment on the bax gene promoter antagonizes p73-dependent apoptosis in costimulated T cells, Cell Death Differ. 15 (2008) 354–363, https://doi.org/10.1038/sj.cdd.4402264.
[14] K.J. Min, S.A. Shahriyar, T.K. Kwon, Arylquin 1, a potent Par-4 secretagogue, induces lysosomal membrane permeabilization-mediated non-apoptotic cell death in cancer cells, Toxicol Res. 36 (2020) 167–173, https://doi.org/10.1007/s43188-019-00025-1.
[15] S.M. Woo, K.J. Min, B.R. Seo, Y.H. Seo, Y.J. Jeong, T.K. Kwon, YM155 enhances ABT-737-mediated apoptosis through Mcl-1 downregulation in Mcl-1-overexpressed cancer cells, Mol. Cell. Biochem. 429 (2017) 91–102, https://doi.org/10.1007/s11010-016-2938-0.
[16] J. Seo, E.W. Lee, J. Shin, D. Seong, Y.W. Nam, M. Jeong, S.H. Lee, C. Lee, J. Song, K6 linked polyubiquitylation of FADD by CHIP prevents death inducing signaling complex formation suppressing cell death, Oncogene 37 (2018) 4994–5006, https://doi.org/10.1038/s41388-018-0323-z.
[17] M. Kucharova, M. Hronek, K. Rybakova, Z. Zadak, R. Stetina, V. Joskova, A. Patkova, Comet assay and its use for evaluating oxidative DNA damage in some pathological states, Physiol. Res. 68 (2019) 1–15, https://doi.org/10.33549/physiolres.933901.
[18] D. Sohn, V. Graupner, D. Neise, F. Essmann, K. Schulze-Osthoff, R.U. Janicke, Pifithrin-alpha protects against DNA damage-induced apoptosis downstream of mitochondria independent of p53, Cell Death Differ. 16 (2009) 869–878, https://doi.org/10.1038/cdd.2009.17.
[19] E. Strom, S. Sathe, P.G. Komarov, O.B. Chernova, I. Pavlovska, I. Shyshynova, D. A. Bosykh, L.G. Burdelya, R.M. Macklis, R. Skaliter, E.A. Komarova, A.V. Gudkov, Small-molecule inhibitor of p53 binding to mitochondria protects mice from gamma radiation, Nat. Chem. Biol. 2 (2006) 474–479, https://doi.org/10.1038/nchembio809.
[20] H. Li, Y. Zhang, A. Strose, D. Tedesco, K. Gurova, G. Selivanova, Integrated high-throughput analysis identifies Sp1 as a crucial determinant of p53-mediated apoptosis, Cell Death Differ. 21 (2014) 1493–1502, https://doi.org/10.1038/cdd.2014.69.
[21] T. Schmidt, K. Korner, H. Karsunky, S. Korsmeyer, R. Muller, T. Moroy, The activity of the murine Bax promoter is regulated by Sp1/3 and E-box binding proteins but not by p53, Cell Death Differ. 6 (1999) 873–882, https://doi.org/10.1038/sj.cdd.4400562.
[22] S. Matsuoka, B.A. Ballif, A. Smogorzewska, E.R. McDonald 3rd, K.E. Hurov, J. Luo, C.E. Bakalarski, Z. Zhao, N. Solimini, Y. Lerenthal, Y. Shiloh, S.P. Gygi, S.J. Elledge, ATM and ATR substrate analysis reveals extensive protein networks responsive to DNA damage, Science 316 (2007) 1160–1166, https://doi.org/10.1126/science.1140321.
[23] G. Xiao, D. Lundine, G.K. Annor, J. Canar, V. Ellison, A. Polotskaia, P. L. Donabedian, T. Reiner, G.F. Khramtsova, O.I. Olopade, A. Mazo, J. Bargonetti, Gain-of-Function mutant p53 R273H interacts with replicating DNA and PARP1 in breast cancer, Cancer Res. 80 (2020) 394–405, https://doi.org/10.1158/0008-5472.CAN-19-1036.
[24] A. Datta, D. Ghatak, S. Das, T. Banerjee, A. Paul, R. Butti, M. Gorain, S. Ghuwalewala, A. Roychowdhury, S.K. Alam, P. Das, R. Chatterjee, M. Dasgupta, C.K. Panda, G.C. Kundu, S. Roychoudhury, p53 gain-of-function mutations increase Cdc7-dependent replication initiation, EMBO Rep. 18 (2017) 2030–2050, https://doi.org/10.15252/embr.201643347.
[25] P.A. Muller, P.T. Caswell, B. Doyle, M.P. Iwanicki, E.H. Tan, S. Karim, N. Lukashchuk, D.A. Gillespie, R.L. Ludwig, P. Gosselin, A. Cromer, J.S. Brugge, O. J. Sansom, J.C. Norman, K.H. Vousden, Mutant p53 drives invasion by promoting integrin recycling, Cell 139 (2009) 1327–1341, https://doi.org/10.1016/j.cell.2009.11.026.
[26] M.R. Bauer, A.C. Joerger, A.R. Fersht, 2-Sulfonylpyrimidines: mild alkylating agents with anticancer activity toward p53-compromised cells, Proc. Natl. Acad. Sci. U. S. A. 113 (2016) E5271–E5280, https://doi.org/10.1073/pnas.1610421113.
[27] J.L. Kaar, N. Basse, A.C. Joerger, E. Stephens, T.J. Rutherford, A.R. Fersht, Stabilization of mutant p53 via alkylation of cysteines and effects on DNA binding, Protein Sci. 19 (2010) 2267–2278, https://doi.org/10.1002/pro.507.
[28] M.R. Fernandez-Fernandez, B. Sot, The relevance of protein-protein interactions for p53 function: the CPE contribution, Protein Eng. Des. Sel. 24 (2011) 41–51, https://doi.org/10.1093/protein/gzq074.
[29] B.W. Schafer, C.W. Heizmann, The S100 family of EF-hand calcium-binding proteins: functions and pathology, Trends Biochem. Sci. 21 (1996) 134–140, https://doi.org/10.1016/s0968-0004(96)80167-8.

[30] L.P. Slomnicki, B. Nawrot, W. Lesniak, S100A6 binds p53 and affects its activity, Int. J. Biochem. Cell Biol. 41 (2009) 784–790, https://doi.org/10.1016/j.biocel.2008.08.007.
[31] M. Grigorian, S. Andresen, E. Tulchinsky, M. Kriajevska, C. Carlberg, C. Kruse, M. Cohn, N. Ambartsumian, A. Christensen, G. Selivanova, E. Lukanidin, Tumor suppressor p53 protein is a new target for the metastasis-associated Mts1/S100A4 protein: functional consequences of their interaction, J. Biol. Chem. 276 (2001) 22699–22708, https://doi.org/10.1074/jbc.M010231200.
[32] S. Rajagopalan, R.S. Sade, F.M. Townsley, A.R. Fersht, Mechanistic differences in the transcriptional activation of p53 by 14-3-3 isoforms, Nucleic Acids Res. 38 (2010) 893–906, https://doi.org/10.1093/nar/gkp1041.
[33] K. Sakaguchi, H. Sakamoto, M.S. Lewis, C.W. Anderson, J.W. Erickson, E. Appella, D. Xie, Phosphorylation of serine 392 stabilizes the tetramer formation of tumor suppressor protein p53, Biochemistry 36 (1997) 10117–10124, https://doi.org/10.1021/bi970759w.
[34] T. Kawaguchi, S. Kato, K. Otsuka, G. Watanabe, T. Kumabe, T. Tominaga, T. Yoshimoto, C. Ishioka, The relationship among p53 oligomer formation, structure and transcriptional activity using a comprehensive missense mutation library, Oncogene 24 (2005) 6976–6981, https://doi.org/10.1038/sj.onc.1208839.
[35] M.R. Fernandez-Fernandez, D.B. Veprintsev, A.R. Fersht, Proteins of the S100 family regulate the oligomerization of p53 tumor suppressor, Proc. Natl. Acad. Sci. U. S. A. 102 (2005) 4735–4740, https://doi.org/10.1073/pnas.0501459102.
[36] W. Lv, B. Su, Y. Li, C. Geng, N. Chen, KIAA0101 inhibition suppresses cell proliferation and cell cycle progression by promoting the interaction between p53 and Sp1 in breast cancer, Biochem. Biophys. Res. Commun. 503 (2018) 600–606, https://doi.org/10.1016/j.bbrc.2018.06.046.
[37] W.C. Chang, J.J. Hung, Functional role of post-translational modifications of Sp1 in tumorigenesis, J. Biomed. Sci. 19 (2012) 94, https://doi.org/10.1186/1423-0127-19-94.
[38] Q. Gan, J. Shao, Y. Cao, J. Lei, P. Xie, J. Ge, G. Hu, USP33 regulates c-Met expression by deubiquitinating SP1 to facilitate metastasis in hepatocellular carcinoma, Life Sci. 261 (2020), 118316, https://doi.org/10.1016/j.lfs.2020.118316.
[39] L. Masclef, O. Ahmed, B. Estavoyer, B. Larrivee, N. Labrecque, A. Nijnik, E.B. Affar, Roles and mechanisms of BAP1 deubiquitinase in tumor suppression, Cell Death Differ. 28 (2021) 606–625, https://doi.org/10.1038/s41418-020-00709-4.
[40] H. Yu, H. Pak, I. Hammond-Martel, M. Ghram, A. Rodrigue, S. Daou, H. Barbour, L. Corbeil, J. Hebert, E. Drobetsky, J.Y. Masson, J.M. Di Noia, B. Affar el, Tumor suppressor and deubiquitinase BAP1 promotes DNA double-strand break repair, Proc. Natl. Acad. Sci. U. S. A. 111 (2014) 285–290, https://doi.org/10.1073/pnas.1309085110.
[41] W. Sime, Q. Niu, Y. Abassi, K.C. Masoumi, R. Zarrizi, J.B. Kohler, S. Kjellstrom, V. A. Lasorsa, M. Capasso, H. Fu, R. Massoumi, BAP1 induces cell death via interaction with 14-3-3 in neuroblastoma, Cell Death Dis. 9 (2018) 458, https://doi.org/10.1038/s41419-018-0500-6.
[42] A. Bononi, C. Giorgi, S. Patergnani, D. Larson, K. Verbruggen, M. Tanji, L. Pellegrini, V. Signorato, F. Olivetto, S. Pastorino, M. Nasu, A. Napolitano, G. Gaudino, P. Morris, G. Sakamoto, L.K. Ferris, A. Danese, A. Raimondi, C. Tacchetti, S. Kuchay, H.I. Pass, E.B. Affar, H. Yang, P. Pinton, M. Carbone, BAP1 regulates IP3R3-mediated Ca(2+) flux to mitochondria suppressing cell transformation, Nature 546 (2017) 549–553, https://doi.org/10.1038/nature22798.
[43] S. Marchi, S. Patergnani, S. Missiroli, G. Morciano, A. Rimessi, M.R. Wieckowski, C. Giorgi, P. Pinton, Mitochondrial and endoplasmic reticulum calcium homeostasis and cell death, Cell Calcium 69 (2018) 62–72, https://doi.org/10.1016/j.ceca.2017.05.003.
[44] S.T. Kim, D.S. Lim, C.E. Canman, M.B. Kastan, Substrate specificities and identification of putative substrates of ATM kinase family members, J. Biol. Chem. 274 (1999) 37538–37543, https://doi.org/10.1074/jbc.274.53.37538.
[45] Z.M. Eletr, L. Yin, K.D. Wilkinson, BAP1 is phosphorylated at serine 592 in S-phase following DNA damage, FEBS Lett. 587 (2013) 3906–3911, https://doi.org/10.1016/j.febslet.2013.10.035.